12 May 86 Conference Presentation

Three-Dimensional Unsteady Flow Fields Elicited by a Pitching Forward Swept Wing

TA 2307-F1-38

J. Ashworth, M. Waltrip, M.W. Luttges

F.J. Seiler Research Laboratory
USAF Academy CO 80840-6528

FJSRL-PR-90-0013

The three-dimensional flow field about a forward swept, NACA 0015 wing was studied using multiple exposure, phase-locked flow visualization viewed from orthogonal perspectives. The wing was oscillated sinusoidally in pitch while stroboscopic photography was used to record the pitching-dependent alterations in flow field structure. Flow interactions were visualized in discrete fashion for a variety of spanwise views, using different k values and mean angles of attack. The major flow field characteristics were the tip and the leading edge vortices. The strong helical tip flow vortices dominate most of the observed flow structures near the wing tip across all test conditions. The far inboard span locations were dominated by flows related to the leading edge vortex. The magnitude and interaction of the flow structures were quite different than the qualitative predictions of previous research. The spatial domain of the flows was quite pronounced and seemed to be specific to the wing geometry of the test configuration.

flow visualization
unsteady flow
vortices

10

UNCLASSIFIED UNCLASSIFIED UNCLASSIFIED NONE

AIAA'86

AIAA-86-1104
Three-Dimensional Unsteady Flow Fields Elicited by a Pitching Forward Swept Wing

J. Ashworth, M. Waltrip and M.W. Luttges,
Univ. of Colorado, Boulder, CO

AIAA/ASME 4th Fluid Mechanics, Plasma Dynamics and Lasers Conference
May 12-14, 1986/Atlanta, GA

THREE-DIMENSIONAL UNSTEADY FLOW FIELDS ELICITED BY A PITCHING FORWARD SWEPT WING

J. Ashworth,* M. Waltrip,* and M.W. Luttges**
Aerospace Engineering Sciences
University of Colorado, Campus Box 429
Boulder, Colorado 80309

Abstract

The three-dimensional flow field about a forward swept, NACA 0015 wing was studied using multiple exposure, phase-locked flow visualization. The flow was viewed from orthogonal perspectives. The wing was oscillated sinusoidally in pitch while stroboscopic photography was used to record the pitching-dependent alterations in flow field structure. Flow interactions were visualized in discrete fashion for a variety of spanwise views, using different K values and mean angles of attack. The major flow field characteristics of the dynamically oscillating swept forward wing were the tip and the leading edge vortices. The strong helical tip flow vortices dominated most of the observed flow structures near the wing tip across all test conditions. And, the far inboard span locations were dominated by flows related to the leading edge vortex. Whereas the swept forward wing elicits flow structures that are qualitatively predictable from previous research, the magnitude and interaction of these flow structures were quite different. The spatial domain of the flows was quite pronounced and seemed to be specific to the wing geometry of the test configuration.

*Graduate Research Assistant, Department of Aerospace Engineering Sciences, Member AIAA

**Professor, Department of Aerospace Engineering Sciences, Member AIAA

Nomenclature

c	wing chord length
d_c	distance from leading edge vortex formation point to shedding or dissipation point, measured along chordline
K	nondimensional reduced frequency parameter, $K=\omega c/2V_\infty$
Re	Reynolds number, $Re = V_\infty c/\nu$
S	nondimensional spanwise distance from wing tip
SZ	leading edge vortex size, measured from wing surface to top of vortical structure (cm)
t	time
t_c	time leading edge vortex is present on top surface of wing
V_c	leading edge vortex convective velocity, $V_c=d_c/t_c$
V_∞	freestream tunnel velocity
x/c	nondimensional distance of vortex center from leading edge, measured along chordline
α	instantaneous wing angle of attack, $\alpha = \alpha_m + \alpha_0 \cos(\omega t)$
α_m	mean angle of attack about which oscillations are centered
α_0	oscillation amplitude
β	spanwise deflection angle at the wing tip (deg.)
Λ	forward sweep angle = 30 degrees
ν	kinematic viscosity
ϕ	nondimensional oscillation phase angle (% cycle beginning at α_{max})
ω	rotational frequency in radians/second

Introduction

Recent advances in the technology of composite structures and in computer-based control systems now permit the use of forward swept wings on high performance aircraft.[1] The swept forward wing configuration is known to perform well at high Mach numbers and has aerodynamic advantages at very low airspeeds.[2] In the aerodynamics arena, considerable work with unsteady separated flows has indicated that such flows can enhance the lifting forces on both two-dimensional airfoils[3,4] and on three-dimensional wings.[5] These two promising new areas of aerospace technology have not been investigated in any combined fashion. To date, the sweep effects of airfoils[6] and delta wings[7] have received only minor attention in regard to unsteady flows. The work described below focuses upon the three-dimensional characteristics of unsteady flows produced about a swept forward wing tested under a variety of dynamic pitching conditions. The complexity of flows known to be produced by lifting surfaces pitching sinusoidally beyond static stall angles[4] dictates the initial use of flow visualization studies. Since the swept forward wing represents a three-dimensional surface and the vortices typical of unsteady flow fields are obviously three-dimensional, comprehensive flow visualizations must allow for full three-dimensional representations. The present study uses a technique reported previously[5] that permits the introduction of smokelines as a single plane that can be followed as it is acted upon by the fluid forces generated by the unsteady separated flows.

Methods

Experiments were conducted in the 40.5 x 40.5 cm low speed wind tunnel at the University of Colorado. The test section walls and top consisted of cast acrylic Plexiglas such that flow could be visualized from any perspective. A small D.C. motor (1/6 h.p.) permitted variable speed driving of a scotch yoik that in turn produced a sinusoidal pitching motion of variable amplitude. Both the driving mechanism and the wing mounting shaft were mounted at a 30° angle relative to the

tunnel test section wall. The induced wing pitching motion was constant throughout the full length of the wing along the lateral axis. Walls not used for specific visualization perspectives were painted flat black to help reduce light reflections. The tunnel velocities were set to achieve Re=30,000 and 40,000.

A hollow core aluminum NACA 0015 airfoil section was used for the wing. The tip was cut parallel to the angle of the oncoming flow. The resulting 30° tip was sealed with a flat plate contoured to the airfoil profile. With these modifications, the effective chord length was 17.6 cm and the thickness-to-chord ratio was 0.13. The oscillation axis around which the wing pitched was 0.22c. By oscillating the wing at frequencies up to 10 Hz, values of K were extended from 0.0 to 1.5. Mean angles of attack were 12, 15 or 18° with the oscillation amplitudes of ±9-10°.

Flow visualization was achieved using a traversing smoke wire technique.[5] The Elgin alloy wire (0.02 cm dia.) introduced a vertical plane of smoke into the flow approximately 2.0c upstream of the wing. As the smokelines passed over the wing, stroboscopic (7 μ sec) illumination was triggered by wing phase angle. Each time the wing passed through the same angles of attack, illumination occurred. The resulting multiple (4-6 flashes) exposure photographs were recorded by a 35mm camera using ASA 400 film. The multiple exposure photographs provided evidence of reliability in the observed flow field structures. To gain an orthogonal perspective, photographs were taken from the side and the top of the wind tunnel test section.

Spanwise positions were examined from the tip of the wing to more inboard sites. These distances were made non-dimensional using chord length. In the oscillation tests, the motion histories began at maximum angles of attack and the full motion cycle was characterized as a percentage of a full cycle.

Results

Flow Visualization in Static Tests

As a basis for dynamic comparisons, the swept forward wing was first examined using flow visualization across a wide range of static angles of attack. To characterize the spanwise perturbation of the resulting flow fields, smoke was allowed to pass over three locations: tip, 0.58c inboard and 1.15c inboard. The flow was photographed from the sideview (tip to root) and from above. In all instances, the photographs used multiple exposure, stroboscopic illumination that assured flow field reproducibility. Angles of attack were varied from 3-27°.

The adherence of the smoke to the contour of the upper surface of the wing was dependent upon the spanwise site visualized. Failure of the smokeline to follow the wing contour was used as evidence of flow separation. At about 3° alpha, flow remained attached at all locations on the wing visualized (Fig.1,Aa). At a static angle of attack of 9°, the most inboard span location visualized (1.15c) began to show indications of flow separation (Fig. 1,b) in contrast to the immediately outboard location (0.58c) where the flow remained attached (Fig. 1,B). When the angle of attack was increased to 15°, above stall for this airfoil, the flow was fully separated inboard and only beginning to separate nearer the wing tip (Fig. 1,Cc). Further increases in the angle of attack (Fig. 1,Dd and 1,Ee) result in more dramatic separations of the flow field from the wing. In all of the visualizations, the separation is less fully developed near the wing tip than it is at more inboard locations.

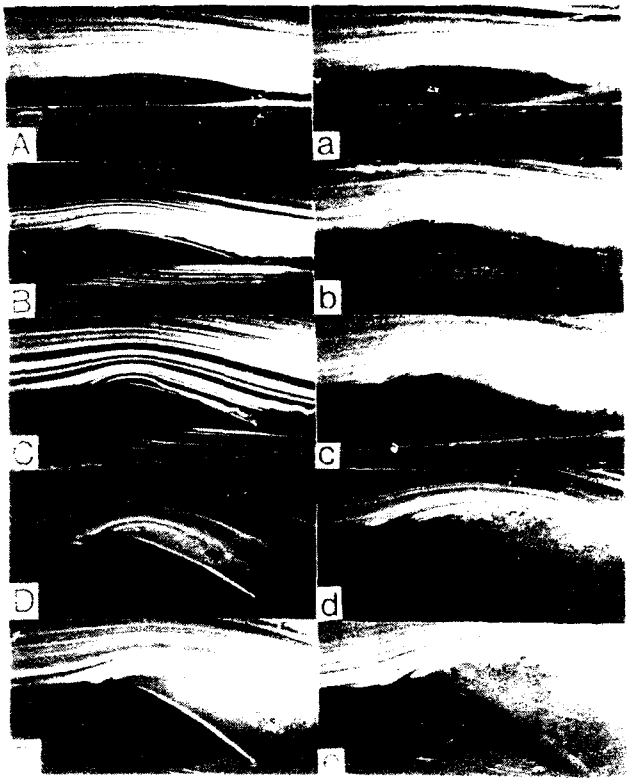

Fig. 1 Spanwise separation on static wing, Re = 40,000, A-E: span location S = 0.58c, a-e: span location S = 1.15c, Aa - Ee: α = 3°, 9°, 15°, 21°, and 27°, respectively.

The flow field visualized at the wing tip was dominated by the presence of a strong helical flow around the tip (Fig. 2,Aa). Across the static angles of attack tested, increased angles were associated with ever tighter helical bending of the smoke around the wing tip. This tightening of the helical flow is formalized in Fig. 3, as the β angle. As can be seen, the positive correlation between the α and β angle persists across all tests and the β angle flattens only at angles of attack associated with inboard flow separation.

When seen from above (Fig. 2), spanwise displacements of the flow are most obvious near the wing tip. The smoke from the upstream smokewire intercepts the wing tip in a manner that pulls the underside flow outward around the tip and then inward over the upper wing surface. The upper surface flow appears to be spatially limited to the span locations very near the tip. At the midspan location (Fig. 2b), the flow is pulled toward the tip by the strong helical tip

vortex. At tested span locations further inboard, the wing tip effect still seems to draw the flow in the direction of the unstalled tip.

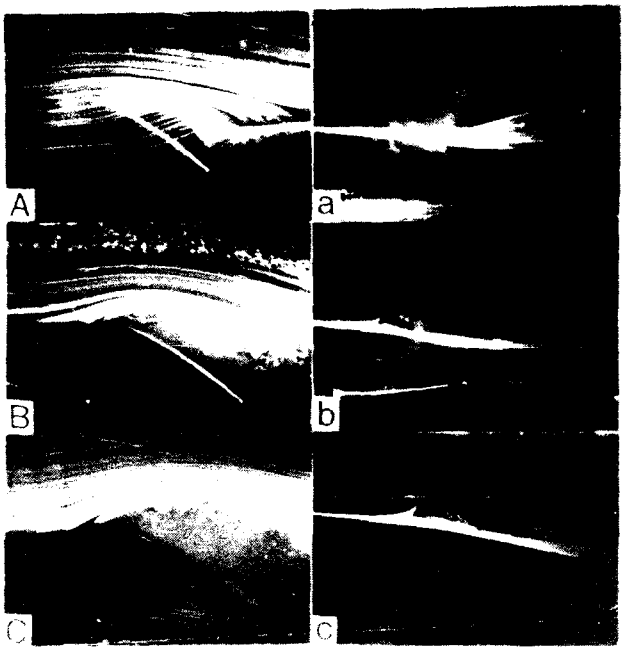

Fig. 2 Spanwise flow displacement on static wing, Re = 40,000, α = 27°, A-C: side view, a-c: top view, Aa: wing tip, Bb: S = 0.58c, Cc: S=1.15c.

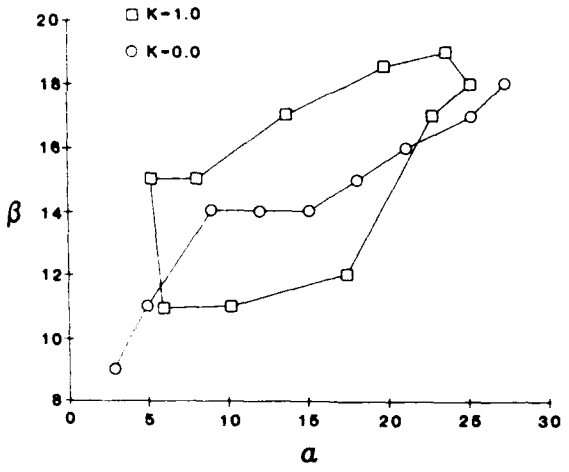

Fig. 3 Tip deflection angle for static and dynamic wing, Re = 40,000, α_m = 15°, α_ω =10°.

Flow Visualization for Pitching Wing Tests

Using multiple exposure, phase-locked photography, the flow field was visualized for the swept forward wing for a variety of K values, mean angles and spanwise locations. Photographs taken stroboscopically at different angles of attack throughout the oscillation cycle produced a record of the resulting flow field. Inevitably, the test conditions yielded vortex dominated flows that varied temporally and spatially both in initiation and development. These variations exhausted the full freedom of the three-dimensional analyses used. Resulting visualizations exhibited considerable reliability, in that the multiple exposures revealed consistently superimposed smoke lines despite the complexity of the elicited flows. This level of reproducibility was clear from both the side and top view visualizations.

Inboard Span Location

At S=1.15c, the span location far inboard from the wing tip, the sinusoidal pitching motions of the wing elicited flow field structures similar to those previously reported for airfoils and flat plates[4] as well as for inboard sites on a straight symmetrical wing[5]. A leading edge vortex was produced as the wing pitched upward through the static stall angle. First appearing in the 0.0 to 0.2 chord location, the vortex grows in apparent size and then begins to convect toward the trailing edge of the airfoil. As the leading edge vortex passed into the wake, only a small amount of evidence of a trailing edge vortex appeared.

Across the test conditions used in these studies, the vortex initiation occurred earlier in the upward pitching motion if the mean angle of attack were increased. When K values were increased, vortex initiation was altered. Also, increased K values yielded higher overall convecting velocities for the passage of the leading edge vortex over the upper airfoil surface and yielded smaller, apparently more cohesive vortex structures. All of these correlates between flow field structure and pitching dynamics are quite similar to those reported earlier[3,4,5]. Accordingly, vortex initiation using 18±9° occurred at 15° on the upstroke but using 12±9°, occurred at 17°. As noted before, earlier vortex initiation was associated with slower average convecting velocities and later initiation was associated with higher convecting velocities. Average convecting velocites tended to mask the fact that earlier initiation yields convection histories characterized by initially slow convection followed later by more rapid acceleration whereas later initiation shows initially modest convection without later accelaration of the vortex to the trailing edge.

Wingtip Location

The wing tip flow about the swept forward wing varied in substantial ways from that observed using a straight symmetrical wing. By characterizing the bending of the smokelines around the wing tip to the upper surface of the wing, β angle, it was possible to quantify the relative characteristics of the wing tip flow throughout a full pitching cycle. A comparison of the angle of tip flow is provided in Fig. 3, for both static tests conducted across a variety of angles of attack and for dynamic tests conducted across pitching motions that moved the wing through the same angles. The dynamic test conditions were α =15±10° with a K value of 1.0. The relatively linear relation between and static angles of attack is displayed and the hysteresis loop of β with dynamic angles of attack is also shown. In the latter case, the angle is small through early stages of the wing upstroke but then increases rapidly through the later stages of the upward piching motion. Near the top of the pitching cycle where α=25°, the associated β angle is greater than that observed during the

static tests at the same angle of attack. The β angles remain larger than those observed for static test counterparts through the downstroke. At the end of the pitching downstroke and the beginning of the upstroke, the wingtip flow is characterized by rapidly decreasing β angle. Once again, the β angle remains small until the midpoint of the upstroke is attained.

This dynamic time history of the wing tip flow correlates well with the inboard initiation, development and convection of the leading edge vortex (Fig. 4). As β angle appears to increase dramatically on the upstroke of the wing, the leading edge vortex is growing over about 0.2 chord inboard. When the β angle is the largest, the vortex has attained mature size and is beginning to convect over the wing surface. The β angle remains elevated over that seen in static tests as long as the leading edge vortex remains over the upper surface of the wing. When the leading edge vortex sheds into the wake of the wing, the β angle drops precipitously to a value smaller than that shown for static tests at the same angle of attack.

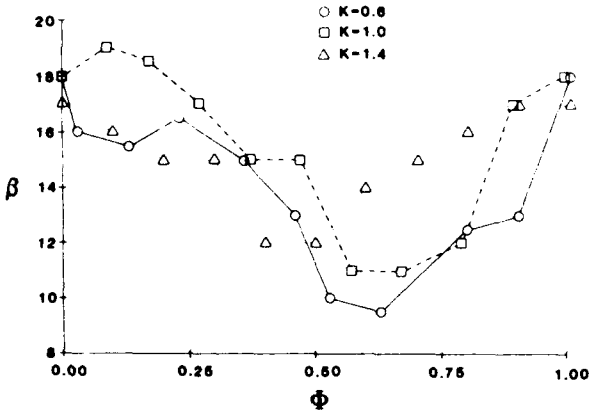

Fig. 4 Tip deflection angles for various K values, Re = 40,000, α_m=15°, α_ω=10°.

Tip vortex flow appears to respond in a systematic manner to alterations in the K values. In the tests that employed K=0.6, the β angles remain low during the wing upstroke until near the maximum angle of attack. Then, the angle of the wing tip flow increases to β values above static test values. The increased β values decrease rapidly but remain at levels higher than the static counterparts through most of the wing downstroke. Notably, the β angles at the lowest angles of attack were quite small at the transition to wing upstroke. These values remain lower than static counterparts throughout much of the upstroke. In contrast, the K=1.4 tests resulted in β values that were routinely higher than static counterparts throughout almost all of the oscillation cycle. The rapid changes in β angles characteristic of tests done with K=1.0 and K=0.6 were absent in the flattened hysteresis loop for the β angles recorded using K=1.4. It is tempting to relate these observations to the fact that a vortex is present over the inboard surface of the wing at all times when a K=1.4.

Midspan Locations

Using the above flow field characteristics as reference points, the flow over the wing between these tip and inboard sites was evaluated. The smoke wire was moved spanwise such that the smoke lines intercepted the wing at points 0.29c, 0.58c and 0.87c inboard of the wing tip. Again, multiple exposure photograghs were taken both from the side and from above the wing. Fig. 5 provides sideview comparisons of flow over some of these spanwise locations for both static and oscillating (K=1.0) wing test conditions where the angle of attack is either constant or instantaneous 18°, respectively. A major difference in the apparent amounts of flow separation is clearly shown for the static as compared to the dynamic test conditions. And, the separation is quite sensitive to spanwise location. Fig. 5 shows a definite separation of the flow from the wing surface in the static tests (B and C) but an attached vortex-initiation flow in the dynamic tests (b and c). At the wing tip a strong vortex is evident in both test cases (Fig. 5A and 5a) and no evidence of flow separation appears. Farther inboard, the flow separation in the static case is preceded upstream about the leading edge of the wing by turbulence whereas in the dynamic case the same site shows the presence of a highly structured vortex (Fig. 5C and 5c).

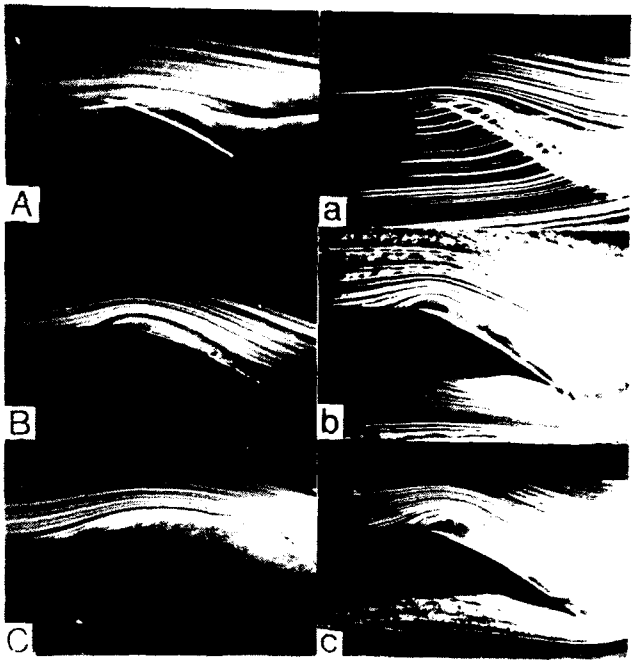

Fig. 5 Side views of static and dynamic wings, Re = 40,000, A-C: static wing, K = 0.0, α =18°, a-c: dynamic wing, K=1.0, α =18°, Aa - Cc: wingtip, S=0.58c and S=1.15c, respectively.

When the same test conditions are visualized from above the wing it is possible to characterize the spanwise deflections of the flow field. Although the spanwise deviations in flow are often complex, an average was obtained by measuring the smoke line displacements at the trailing edge of the wing from the initial plane of smoke introduction upstream of the leading edge. In this way it was possible to evaluate the spanwise flow of both the upper and lower surface

smoke lines. The resulting measures were collected and summarized for each set of test conditions. These summaries were helpful in interpreting the data reported here, but will not be formally presented.

The apparent size of the leading edge vortex previously has been reported to be inversely related to the magnitude of the K value.[4] In tests with the swept forward wing, this relationship appears to be strongly related to the spanwise site of the observations (Fig. 6). At S=1.15c the vortex size is inversely related to K value. At S=0.87c the vortex size changes very little with alterations in K value. And at S=0.58c or S=0.29c, the vortex size actually increases with increasing K values. At these sites closer to the wing tip, the vortex forms and grows near the leading edge but then the vortex structure dissipates as it begins to move toward the trailing edge of the wing. Despite these variations in growth dynamics related to K values, it remains clear that the leading edge vortices are very much smaller near the wing tip than at inboard locations on the span.

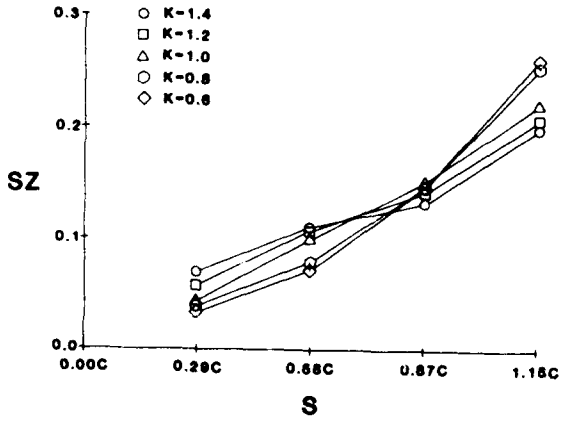

Fig. 6 Leading edge vortex size, Re = 40,000, α_m = 15°, α_ω =10°.

The convection velocities, V_c, were calculated as average values for the time of vortex appearance near the leading edge to the time of shedding from the trailing edge. Or, it was calculated from the time of appearance to the time of structure dissipation. This method includes both the initiation and formation times for the vortex; times when the vortex appears not to move over the surface of the wing. In all cases, the vortex was observed to convect slowly over the leading portions of the chord and more rapidly over the downstream chord locations. The influence of span location on V_c is summarized in Fig. 7. The progressive acceleration of the vortices for different span locations is summarized across the chord of the wing throughout an oscillation cycle in Fig. 8. Regardless of span location, increases in K were associated with higher V_c values. And, the more inboard locations on the span also were associated with higher V_c's. To better summarize these observations, the positions of the vortices over the wing are plotted on the wing planform for different portions of the pitching cycle, 0.0, 0.25 and 0.50, in Fig. 9.

The mean angles of attack around which the sinusoidal motions of the wing were driven were

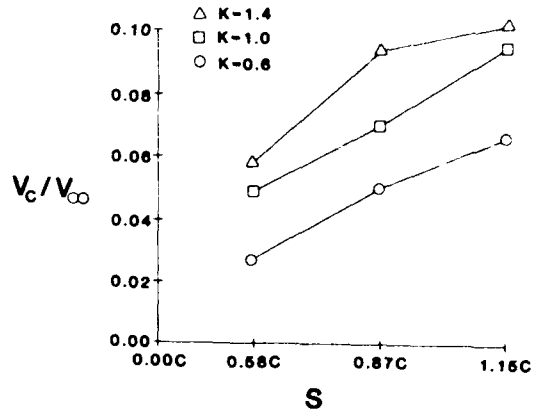

Fig. 7 Convective velocities, Re = 40,000, α_m=10°.

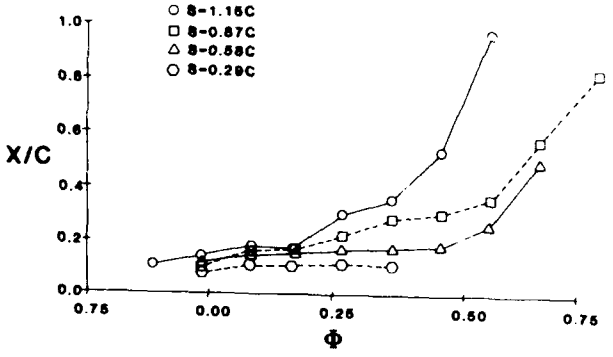

Fig. 8 Leading edge vortex position along the chordlength, Re = 40,000, K = 1.0, α_m=15°, α_ω =10°.

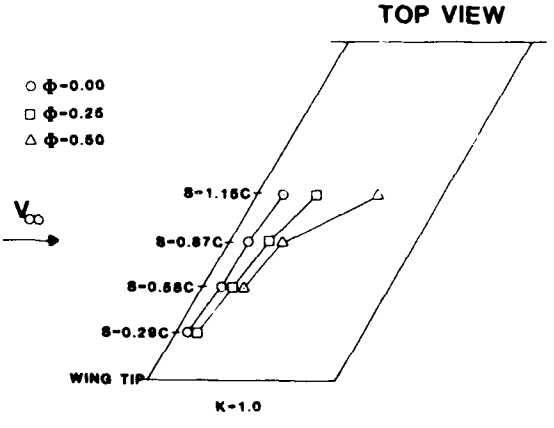

Fig. 9 Planform leading edge vortex position, Re = 40,000, K = 1.0, α_m=15°, α_ω=10°, ϕ=0 α=25°, ϕ=.5 α=5°.

varied between 12, 15 and 18° using motions of ±9-10°. The leading edge vortex formation occurred earlier in the upward pitching motion when the mean angle of attack was increased (Fig. 10) and when the observation site was S=1.15c. At a span location closer to the tip (S=0.58c), the initiation of vortices was delayed until later in the upward pitching motion cycle. But, the higher mean angles of attack led to more delay in the vortex initiation. In this instance it

appeared that the effect of the mean angle of attack on tip vortex flow was greater than it was on inboard flow; thus the inboard flow was clearly influenced by high angle of attack strengthening of wing tip flow. Coupled to the differences in vortex initiation, the overall V_c was lower for lower mean angles of attack. As may be seen in Fig. 11, the low V_c values derive from earlier vortex initiation with high mean angles of attack. It is equally clear that higher mean angles eventually produce greater vortex convection than lower angles when the whole oscillation cycle is considered. Inboard (S=1.15c) vortices traveled faster and further than outboard (S=0.58c) vortices as indicated by the planform plots of Fig. 12. These observations are not to be confused with the initiation phenomena presented above.

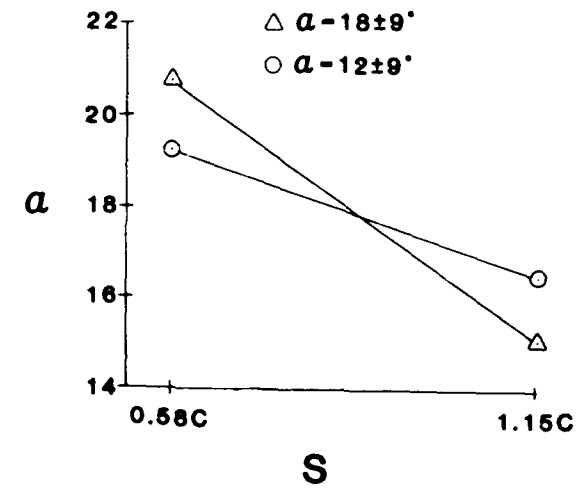

Fig.10 Leading edge vortex initiation point, Re = 40,000, K = 1.0, α_m=12° and 18°, α =9°.

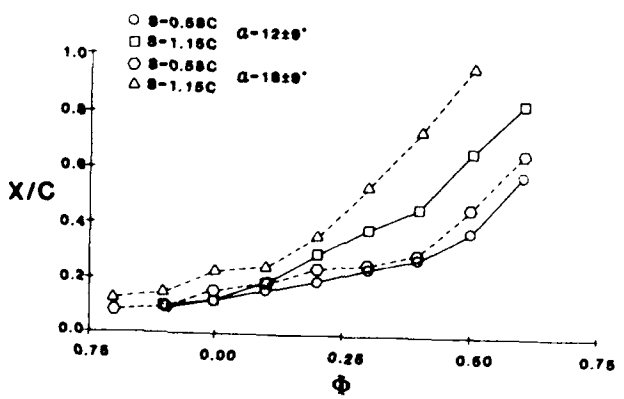

Fig.11 Leading edge vortex position, Re = 40,000, K = 1.0, α_m=12° and 18°, α =9°.

One manner for comparing the interaction between the tip and inboard flow patterns elicited on the pitching wing is to compare signature characteristics of each across a full oscillation cycle. The data presented in Fig. 13 show a comparison between the β angle of wing tip flow and vortex size, SZ, measured at S=0.29c inboard. When the vortex is apparent inboard, the tip β angle is large. When the inboard vortex has dissipated, the β angle is at minimum value. Variations between these extremes show a very high correlation between changes in β angle and changes in vortex size across the whole oscillation cycle. In these studies no causal relationship was tested but it appears clear that such relations deserve further attention.

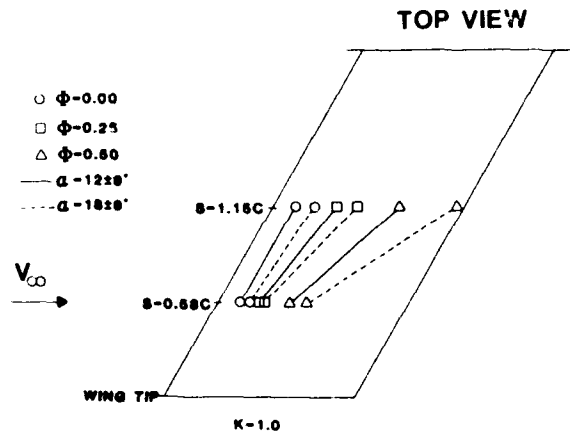

Fig.12 Planform leading edge vortex position, Re = 40,000, K = 1.0, α_m=12° and 18°, α =9°.

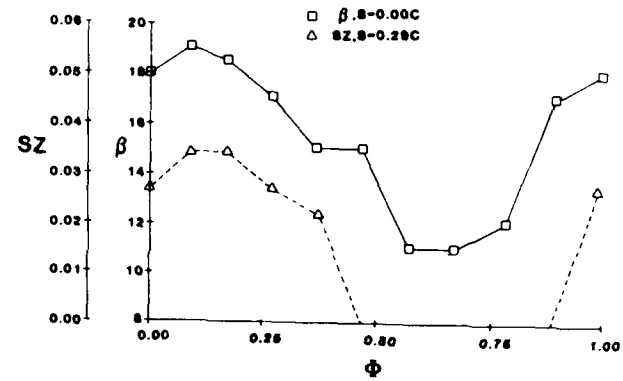

Fig.13 Wing tip deflection angle and leading edge vortex size comparison, β at S=0.0, SZ at S = 0.29c, Re = 40,000, K = 1.0, α_m=15°, α =10°.

Multiple Vortices and Flow Elaboration

Two leading edge vortices were always observed during certain test conditions and at specific sites on the wing (Fig. 5). Other flow structures such as the appearance of another vortex and the appearance of an apparent shear layer also were reliably observed. The two vortices that were produced during a single upward pitching motion are shown in Fig. 14. They appear one after the other in time and chord location. The main vortex forms in the usual fashion on the upstroke with the secondary vortex appearing slightly later and slightly downstream. The secondary vortex is only half or two-thirds the apparent size of the primary vortex but has the same rotational sense. The secondary vortex, formed downstream, convects more rapidly toward the trailing edge of the wing than the primary vortex. Thus, the two vortices appear to pull apart once they have formed. Consistent with previously described flow behavior, the tandem vortices were only seen briefly over the upstream chord locations at S=0.58c. As may be seen in Fig. 15B

and 15C, the shedding of the secondary vortex coincides with the appearance of a tertiary vortex upstream of the primary vortex. The tertiary vortex appears to rotate with the same sign as both the primary and secondary vortices. If this vortex appeared, it traversed the whole chord of the wing immediately ahead of the primary vortex. Further toward the tip, a variety of other structures appeared quite transiently and shear layer flows appeared to be in evidence.

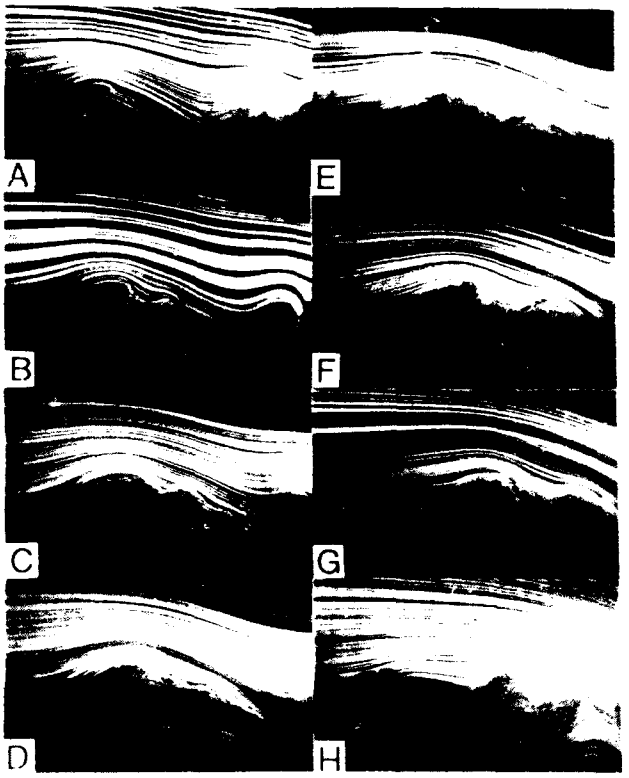

Fig.14 Progression of second vortical structure, Re=30,000, K=1.5, S=1.15c, A-H: α=25°, 23°, 18°, 12°, 7°, 5°, 7° and 12° respectively.

Discussion

The swept forward wing yielded unsteady separated flow fields that in many ways were reminiscent of those three dimensional flows elicited by a symmetric wing.[3,5] Of critical comparative importance was the failure of tip vortices to decrease in apparent strength at very high angles of attack and the stalling characteristics whereby the inboard regions of the span stall at lower angles of attack than the tip regions. These static angle of attack dependencies undoubtedly contributed to the dynamic pitching characteristics exacted on the flow field.

The effects of K values and mean angles of attack on inboard, leading edge vortices were well behaved. With increased K these vortices formed later in the upward pitching motion and with increased mean angles of attack the vortices were formed earlier. Vortex initiation point was correlated with V_c in that earlier initiation invariably led to lower V_c values and later initition, to higher V_c values. Apparent vortex size was inversely related to the V_c values.

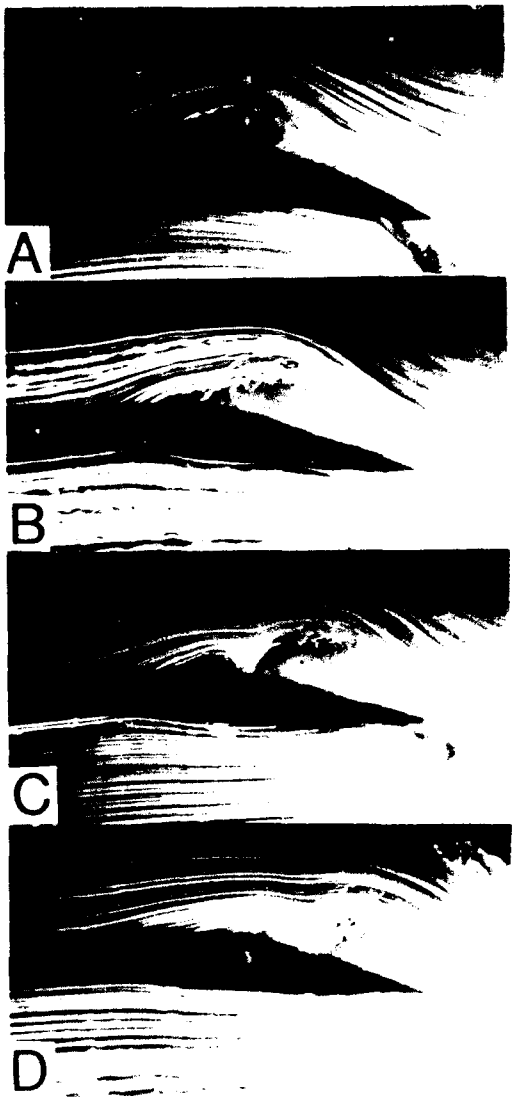

Fig.15 Formation of third leading edge vortex, Re=40,000, K=1.2, S=1.15c, A-D: α =12°, 7°, 5° and 7°, respectively.

At the wing tip the curvature of flow inboard was determined both by angle of attack and by the presence or absence of a leading edge vortex. As the wing pitched through a complete cycle, the wing tip flow curvature showed significant amounts of hysteresis and significantly more magnitude than observed during static angle of attack tests. The hysteresis was most clear during low K value tests and the overall magnitude of curvature was most obvious using high K values.

The interaction between these flow patterns was spatially dependent upon span location and temporally dependent upon pitching characteristics of the wing. In the former case, flows near the tip over the wing developed more slowly than inboard flows. The resulting vortices were more capricious,[9] the apparent V_c values smaller, and the vortices disappeared before reaching the trailing edge. As a result of higher K values, vortex flows near the tip were delayed in the pitching cycle to initiation at higher angles of attack and the apparent vortex size (small in comparison to inboard vortices) was increased. At high K values, the primary vortex was joined by additional vortices during a single pitching

motion. Planform plots reveal two disparate regions on the upper surface of the wing that are the domains of leading edge vortices or tip vortices, respectively. The leading edge vortex domain consists of a triangular wedge with the base far inboard and the apex near the leading edge of the wing tip. One side of the wedge is outlined by the leading edge of the wing and the other side is generally bounded by a line beginning at the trailing edge inboard and running to the front of the wing tip. In contrast, the domain of the tip flow structures is a distorted wedge shaped area bounded by the tip and by a line beginning from the leading edge of the tip and passing to the trailing edge of the wing where a base is formed. Between these domains is the area on the wing where a variety of flow field structures arise, presumably from the interactions of the leading edge and wing tip vortices. Such interactions appear to affect the magnitude of existing flow field structures rather than the qualitative nature of the flow fields. Thus, the wing tip domain is characteristically that of the wing tip vortex where inboard flows change the angle but not the overall flow field. And, the leading edge vortex domain shows a vortex that responds to tip flow but this vortex is not lost to the tip flow effects.

The specific contributions of the swept forward wing to the three-dimensionality of the flow field during pitching appear to arise from a combination of the inboard stalling characteristics of the wing at high angles of attack and the reluctance of the tip to show stall at such high angles. In addition, the two flow field domains described above interact in a non-orthogonal fashion due to the forward sweep of the wing.

The result of these swept forward wing interactions is most evident in the growth of the leading edge vortex near the wing tip. Unlike previously reported instances in which increases in K value result in decreased vortex sizes, the vortex size near the wing tip actually increases with increased K values. In fact, this relationship only exits in flow regions near the wing tip. Further inboard, the size of the leading edge vortex behaves as it does in two-dimensional airfoil tests. Coupled with this observation is the alteration in the character of the helical tip vortex. The vortex shows exaggerated angles across all dynamic test conditions but the exaggeration is neither as large nor as influenced by hysteresis as in tests using a straight symmetrical wing.

Conclusions

The forward swept wing statically and dynamically produced flow fields that differed significantly from those reported for a straight symmetric wing.[5] In the static tests, the inboard span of the wing stalled at lower angles of attack than outboard span areas. The flow about the wing tip did not separate even at angles of attack approaching 30°. These characteristics have been the subject of a previous investigation.[2] In dynamic pitching tests, the swept forward wing differed from the symmetric wing primarily in regard to the manner in which the leading edge vortex developed along the span. The development of inboard vortices occurred at lower angles of attack than that of tipward vortices, across all K values and mean angles of attack. Areas along the span of interacting tip and leading edge vortices show more flow field capriciousness than was evident using a symmetric wing.

As observed earlier using two-dimensional airfoils and plates,[3] as well as a three-dimensional wing,[5] increases in K value result in leading edge vortex appearance at higher angles of attack in the upward pitching motion. This delay is invariably matched by higher V_c values. Opposite effects are seen for increases in the mean angles of attack around which pitching occurs. Within approximately 0.5c of the wing tip the relationships appear to reverse in that higher K values result in more vortex size and slower apparent V_c. At these span locations increases in mean angle do not ameliorate the effects of K value.

It is interesting to note that previous studies have shown that airfoil and plates across a variety of Re numbers elicit quite similar dynamic flow field changes.[4] The upward motion generates a leading edge vortex that passes over the chord to the trailing edge. Depending upon K value, a trailing edge vortex is elicited with opposite sign. This trailing edge vortex often causes a rapid separation of the flow from the airfoil surface. Such conditions are associated with "cataclysmic" stall. In the present studies there was little evidence for the presence of a trailing edge vortex and dramatic flow separation was not coincident with the passage of the leading edge vortex into the wake.

The work of Gad-el-Hak and his colleagues[7] and that of Carta[6] shows that the swept back and delta wings also seem to have little evidence of a trailing edge vortex. Both series of investigations suggest that vortices form over the upper surfaces at high angles of attack and that these vortices simply increase or decrease in size as pitching is introduced. In these reported instances it is easy to imagine that an induced leading edge vortex simply adds to the existing vortices over the two different test surfaces.

Recent work by Freymuth and his colleagues[8,9] gives a rather suggestive view of the three-dimensional vorticity that supports some of the flow field structures observed here and previously using swept forward and symmetric wings[3,4,5] respectively. In a recent study (these proceedings), a symmetric wing was marked with $TiCl_4$ just prior to initiating a flow that accelerated linearly from rest to approximately 40 ft per sec. The vorticity of both the wing tip and the leading edge was evident. Across a wide range of angles of attack the vorticity accumulated across the leading edge in a pattern like that described above for the area that supports the pitch-induced vortices. The tip vorticity showed a pattern reminiscent of that described for the helical pattern of the tip vortex above. Between these two areas there was no apparent accumulation of vorticity. Higher angles of attack in the acceleration experiments resulted in areas of vorticity that appear to converge over the surface of the wing, but these two areas do not exhibit complete convergence. It

seems possible that the upward pitching swept forward wing tested in the above experiments brings underlying areas of vorticity close together as in Freymuth's experiments. The resulting flow field, accordingly, might be expected to show the elaboration actually observed in the present experiments.

The present experiments show that unsteady separated flows can be reliably produced about a swept forward wing. The pitching dynamics of the wing yielded predictable alterations in vortex initiation, development, V_c and shedding. The aerodynamic forces that are associated with these flow field observations are yet to be determined. However, it appears that the manner in which the underlying vorticity supports the flow field structures may be quite uniform and, eventually, predictable.

Acknowledgements

This work was supported, in part, by the U.S. Air Force Office of Scientific Research, Grant F4962083K0009, Dr. James McMichael, project manager. The technical assistance of W. Bank, R. Meirzer, S. Walts, J. Myers and J. Button is appreciated.

References

1. Moore, M. and Frei, D. "X-29 Forward Swept Wing Aerodynamic Overview". AIAA 83-1834, AIAA Applied Aerodynamics Conference. Danvers, Massachusetts, July, 1983.

2. Uhad, G. C., Weeks, T. M. and Lange, R. "Wind Tunnel Investigation of Transonic Aerodynamic Characteristics of Forward Swept Wings". J. Aircraft, 20(3): 195-202, March, 1983.

3. Mc Croskey, W. J. "Unsteady Airfoils". Ann. Rev. of Fluid Mech., 1982. pp 285-311.

4. Robinson, M. C. and Luttges, M. W. "Unsteady Separated Flow: Forced and Common Vorticity About Oscillating Airfoils". Workshop on Unsteady Separated Flows, Francis, M. and Luttges, M. (eds.). Univ. Colorado: 1984. pp 117-126.

5. Adler, J. and Luttges, M. "Three-Dimensionality in Unsteady Flow About a Wing". AIAA 85-0132, AIAA 23rd Aerospace Sciences Meeting, Reno, Nevada, Jan. 1985.

6. Carta, F. O. "Unsteady Stall Penetration of an Oscillating Swept Wing". Workshop on Unsteady Separated Flows, Francis, M. and Luttges, M. (eds.), Univ. Colorado: 1984. pp 28-37.

7. Gad-el-Hak, M., Ho, C. and Blackwelder, R. F. "A Visual Study of a Delta Wing in Steady and Unsteady Motion". Workshop on Unsteady Separated Flows. Francis, M. and Luttges, M. (eds.), Univ. Colorado: 1984. pp 45-51.

8. Freymuth, P., Bank, W. and Palmer, M., "Vortices Around Airfoils". Amer. Sci., 72, 242-248, 1984.

9. Freymuth, P., "The Vortex Patterns of Dynamic Separation: A Parametric and Comparative Study". Prog. Aerospace Sci., Vol. 22, 1985, pp. 161-288.

-- NOTES --